Brassicaceae-specific Gretchen Hagen 3 acyl acid amido synthetases conjugate amino acids to chorismate, a precursor of aromatic amino acids and salicylic acid

Cynthia Holland, Corey Westfall, Jason Schaffer, Alejandro de Santiago, Chloe Zubieta, Sophie Alvarez, Joseph Jez

JBC Papers in Press. Published on October 1, 2019 as Manuscript RA119.009949
The latest version is at http://www.jbc.org/cgi/doi/10.1074/jbc.RA119.009949

Brassicaceae-specific Gretchen Hagen 3 acyl acid amido synthetases conjugate amino acids to chorismate, a precursor of aromatic amino acids and salicylic acid

Cynthia K. Holland[1], Corey S. Westfall[1], Jason E. Schaffer[1], Alejandro De Santiago[1], Chloe Zubieta[2], Sophie Alvarez[3], and Joseph M. Jez[1*]

From the [1]Department of Biology, Washington University, St. Louis, MO 63130, USA; [2]Laboratoire de Physiologie Cellulaire & Végétale, Univ. Grenoble Alpes, CNRS, CEA, INRA, IRIG, Grenoble, France; [3]Department of Agronomy and Horticulture, University of Nebraska-Lincoln, Lincoln, NE 68583, USA

**Corresponding author; E-mail: jjez@wustl.edu*

Running title: AtGH3.7 and AtGH3.12 conjugate amino acids to chorismate

Keywords: *Arabidopsis thaliana*, chorismate, crystal structure, Gretchen Hagen 3, plant defense, salicylic acid, aromatic amino acid, phytohormone, AtGH3.12, AtGH3.7

To modulate responses to developmental or environmental cues, plants use Gretchen Hagen 3 (GH3) acyl acid amido synthetases to conjugate an amino acid to a plant hormone, a reaction that regulates free hormone concentration and downstream responses. The model plant *Arabidopsis thaliana* has 19 GH3 proteins, of which 9 have confirmed biochemical functions. One Brassicaceae-specific clade of GH3 proteins was predicted to use benzoate as a substrate and includes AtGH3.7 and AtGH3.12/PBS3. Previously identified as a 4-hydroxybenzoic acid-glutamate synthetase, AtGH3.12/PBS3 influences pathogen defense responses through salicylic acid. Recent work has shown that AtGH3.12/PBS3 uses isochorismate as a substrate, forming an isochorismate-glutamate conjugate that converts into salicylic acid. Here, we show that AtGH3.7 and AtGH3.12/PBS3 can also conjugate chorismate, a precursor of aromatic amino acids and salicylic acid, to cysteine and glutamate, respectively. The X-ray crystal structure of AtGH3.12/PBS3 in complex with AMP and chorismate at 1.94 Å resolution, along with site-directed mutagenesis, revealed how the active site potentially accommodates this substrate. Examination of Arabidopsis knockout lines indicated that the *gh3.7* mutants do not altered growth and no increased susceptibility to the pathogen Pseudomonas syringae, unlike *gh3.12* mutants, which ere more susceptible than wild-type plants, as was the *gh3.7/gh3.12* double mutant. The findings of our study suggest that GH3 proteins can use metabolic precursors of aromatic amino acids as substrates.

Plants have adapted and evolved a number of chemicals to respond to the world around them (1). By modifying common growth and defense hormones, plants are able to activate or inactivate hormone molecules rapidly in response to environmental cues (2-3). One set of phytohormone modifying enzymes are the Gretchen Hagen 3 (GH3) family of acyl acid amido synthetases. These enzymes conjugate

amino acids to acyl acids, notably the plant hormones indole-3-acetic acid (IAA; the major auxin hormone) and jasmonic acid (2, 4). In some cases, the amino acid-conjugated hormone is a storage or degradation form of the molecule, but in other cases, the conjugate is the active form of the molecule that binds the hormone receptor (5-7).

Although GH3 proteins are found in all plants, the roles of many of these proteins remains to be investigated. In *Arabidopsis thaliana* (thale cress), there are 19 GH3 proteins, and to date, only 8 of these have been biochemically characterized - AtGH3.1, AtGH3.2, AtGH3.3, AtGH3.5/WES1, AtGH3.11/JAR1, AtGH3.12/PBS3, AtGH3.15, and AtGH3.17/VAS2 (8-13). Using the x-ray crystal structures of AtGH3.11 and AtGH3.12, the acyl acid substrate binding pocket was compared to determine the active site residues across all GH3 proteins (10). With this information, the function of a given GH3 protein can be predicted based on the known function of GH3 proteins within that clade.

The largest clade of GH3 proteins modify and inactivate the primary auxin IAA and includes the well-studied AtGH3.1, AtGH3.2, AtGH3.3, AtGH3.5/WES1, and AtGH3.17/VAS2 proteins (9-11). The second largest clade contains AtGH3.11/JAR1 and related proteins from multiple plants that function as jasmonyl-isoleucine synthetases to produce the bioactive jasmonate hormone (8, 10). Recently, AtGH3.15 was found to modify the auxin precursor indole-3-butyric acid and auxin herbicides suggesting a role for GH3 proteins outside of the canonical plant hormones (12-13).

Another clade of GH3 proteins with a characterized homologue is Brassicaceae-specific and has two members in Arabidopsis - AtGH3.7 and AtGH3.12/PBS3, which share 75% amino acid sequence identity (10). AtGH3.12/PBS3 was originally identified in a mutant screen for increased susceptibility to both avirulent and virulent *Pseudomonas syringae* strains and was named *pbs3-1* (*avrPphB susceptible 3*) (14). Later work identified a biochemical activity with the non-physiological substrate 4-hydroxybenzoic acid (4-HBA) (15). In Arabidopsis, knockout of *pbs3* resulted in reduced levels of salicylic acid (SA), a plant pathogen defense signaling molecule, and showed decreased accumulation of pathogen responsive gene transcripts and SA-glucosides after infection (15-17). While SA biosynthesis is predicted to occur in the chloroplast (18-20), SA-glucosides can be actively transported to the vacuole, where these molecules presumably function as a storage form of SA (21-23). Interestingly, treatment of *pbs3-1* plants with exogenous SA leads to normal induction of pathogen responsive transcripts and SA-glucosides after infection and the SA-treated *pbs3-1* plants are as resistant to *P. syringae* infection as wild-type plants (17). From these studies, it was proposed that AtGH3.12/PBS3 functions upstream of SA, potentially in its biosynthesis. Recent work identified a plastidial membrane transporter and AtGH3.12/PBS3 as required proteins in SA production (24). In that study (24), AtGH3.12/PBS3 forms an isochorismate-glutamate conjugate, which degrades into SA. This work also identified chorismate-glutamate as a secondary product of the enzyme (24). To date, AtGH3.7, the other member of this clade, has escaped *in vivo* and biochemical characterization.

SA can be synthesized by two routes in plants, both of which use the aromatic amino acid branchpoint metabolite, chorismate, as a precursor (25). In one pathway, the chorismate-derived aromatic amino acid phenylalanine is converted into SAthrough benzoate intermediates or coumaric acid (26). The second pathway converts chorismate into SA using isochorismate synthase and AtGH3.12/PBS3 (18, 27). There are two *isochorismate synthase* genes in Arabidopsis, but the *ics1/ics2* double mutant line still

produces SA, suggesting that this pathway is not the only source of SA in this model plant (20). AtGH3.12/PBS3 forms isochorismate-glutamate, which then degrades into SA (24); however, homologs of AtGH3.12/PBS3 and AtGH3.7 are only found in the Brassicaceae (10), which raises a question of how widespread this new biosynthetic pathway actually is in the plant kingdom.

Here, we re-examined the possible biochemical function of the Brassicaceae-specific clade proteins AtGH3.12/PBS3 and AtGH3.7 and, in the absence of commercially available isochorismate, identified each protein as chorismate-conjugating enzymes. Using a combination of steady-state kinetics, x-ray crystallography, and site-directed mutagenesis, the molecular basis of chorismate binding in AtGH3.12/PBS3 was revealed, which also provides insight on the isochorismate-conjugating activity of this protein. The *in vivo* role of AtGH3.7 was analyzed through *P. syringae pv. tomato* DC3000 infection assays, and a double mutant *gh3.7/gh3.12* Arabidopsis line was generated to determine the combined role of this unique class of GH3 proteins in the Brassicaceae family. Due to the relaxed substrate specificity that is typical of GH3 proteins, it is not surprising that AtGH3.12/PBS3 can recognize both chorismate and isochorismate as substrates (11-13, 24).

RESULTS

Identification of chorismate-conjugation by AtGH3.12/PBS3 and AtGH3.7

Previously, AtGH3.12/PBS3 (At5g13320; NP_196836.1) was implicated in pathogen defense; however, its biochemical function was left unclear until recently, as only 4-HBA, a non-physiological substrate, was originally identified as a substrate for conjugation with glutamate (15-16, 24). No studies of AtGH3.7 (At1g23160; NP_173729.1) have been reported. Here, both proteins were recombinantly expressed in *Escherichia coli* and purified using Ni^{2+}-affinity and size-exclusion chromatography. To identify a possible physiological substrate, we used a coupled assay that measures AMP release from the second half-reaction (10) and a matrix-panel of 15 acyl acid hormones and hormone intermediates (4-HBA, benzoic acid, IAA, phenylacetic acid, SA, indole-3-butyric acid, gibberellic acid, abscisic acid, anthranilate, shikimate, chorismate, prephenate, 4-hydroxyphenylpyruvate, cinnamic acid, and *p*-coumaric acid) and the 20 proteogenic amino acids. Because isochorismate is not commercially available, it was not included in our matrix-panel.

Screening of AtGH3.12/PBS3 confirmed the previously identified activity for the conjugation of 4-HBA, as well as benzoic acid, prephenate, and *p*-coumaric acid, with glutamate (**Fig. 1a**) (10, 15-16); however, activity for the enzyme as a chorismate-conjugating enzyme was identified with a specific activity 8-fold higher than that determined for 4-HBA (**Fig. 1a**). No activity was observed with the other acyl acid/amino acid combinations. Formation of the chorismate-glutamate conjugate formed by AtGH3.12/PBS3 was confirmed by LC-MS/MS. Incubation of the enzyme with chorismate, ATP, and glutamate led to formation of a peak with a *m/z* of 353.9, which matches the expected deprotonated chorismate-glutamate conjugate (**Fig. 2**). As a negative control, assays in the absence of protein or any one substrate did not lead to observation of the product peak. AtGH3.12/PBS3 displayed the highest specific activity using glutamate as the amino acid substrate (2,400 nmol min^{-1} mg $protein^{-1}$; **Fig. 1b**), which is consistent with earlier reports of this proteins second half-reaction specificity (10, 15-16). This activity was 4.5-fold higher than the next highest specific activity, which was with leucine (520 nmol min^{-1} mg^{-1}).

Steady-state kinetic analysis of

AtGH3.12/PBS3 revealed similar K_m values for 4-HBA (270 μM) and chorismate (170 μM), but the turnover rate for chorismate was nearly 10-fold higher than that observed for 4-HBA (**Table 1**). This leads to chorismate having a roughly 15-fold higher catalytic efficiency (k_{cat}/K_m) than 4-HBA (4,220 M^{-1} s^{-1} and 278 M^{-1} s^{-1}, respectively).

The activity of AtGH3.12/PBS3 with chorismate as substrate led us to examine AtGH3.7, the other enzyme in the same clade that shares a conserved acyl acid binding site with AtGH3.12/PBS3 (10). Using the same panel of acyl and amino acid substrates, the chorismate conjugating activity of AtGH3.7 was identified with the highest activity observed using cysteine as the amino acid substrate (**Fig. 3a**). The specific activity of AtGH3.7 with chorismate was ~50-fold higher than that of either *p*-coumaric and cinnamic acid substrates. No activity with other acyl acids in the panel was observed. Screening of the chorismate conjugation with each amino acid identified the highest activity with cysteine as a substrate, along with serine and glutamine as possible other substrates (**Fig. 3b**). Steady-state kinetic analysis of AtGH3.7 indicates that the chorismate and cysteine substrate pair is the preferred combination compared to either serine or glutamine as the amino acid substrate (**Table 2**). Compared to AtGH3.12/PBS3, AtGH3.7 shows a comparable K_m value and a 2-fold lower turnover rate, which results in protein that is 3-fold less efficient than AtGH3.12/PBS3 for conjugating chorismate (**Table 2**). Of the 20 amino acids, cysteine, serine, and glutamine had the highest activities, but further kinetic analysis showed that the preferred amino acid substrate is cysteine (**Table 2**). With cysteine, saturation kinetics was observed, but kinetic analysis with both serine and glutamine displayed linear behavior up to 10 mM concentrations. This indicates that the Km values for these amino acids are substantially higher and not in a physiologically relevant range.

The identification of chorismate-conjugating activity of these two GH3 proteins led us to re-examine why this activity was missed in previous studies, which used a phosphate-release assay to monitor the first-half reaction (i.e., adenylation) activity of AtGH3.12/PBS3 (15). To understand the failure of the adenylation assay in detecting the chorismate activity, we repeated the assay in the absence and presence of glutamate (**Fig. 4**). Using this assay in the absence of an amino acid, AtGH3.12/PBS shows a higher specific activity with 4-HBA than with chorismate (120 ± 4 nmole min^{-1} mg^{-1} and 24 ± 1.2 nmole min^{-1} mg^{-1}, respectively), as previously observed (15). Addition of glutamate to the assay mix leads to a modest increase in adenylation rate with 4-HBA (140 ± 1.5 nmole min^{-1} mg^{-1}). In contrast, the observed activity with chorismate increases 35-fold (620 ± 14 nmoles min^{-1} mg^{-1}) (**Fig. 4**).

Salicylic acid (SA) inhibition of chorismate conjugate formation in AtGH3.12/PBS3 and AtGH3.7

Previously published AtGH3.12/PBS3 kinetic data showed that SA was a competitive inhibitor in the reaction with 4-HBA (15). With the new data showing that 4-HBA is not the preferred substrate of AtGH3.12/PBS3, we wanted to confirm that the reaction was still inhibited with by SA when chorismate was the acyl acid substrate. SA inhibited AtGH3.12/PBS3 with an IC_{50} of 7 ± 1 μM, which is similar to what was found previously with 4-HBA as a substrate (IC_{50} = 15 μM; ref. 15). Because AtGH3.7 also uses chorismate as a substrate, we hypothesized that chorismate-cysteine conjugate formation by AtGH3.7 would also be inhibited by SA. In contrast to AtGH3.12/PBS3, SA less effectively inhibited AtGH3.7 with an IC_{50} value of 2.4 ± 0.2 mM, which is 340-fold higher than the IC_{50} value of SA for AtGH3.12/PBS3 with chorismate as an acyl

acid substrate.

Structural analysis of AtGH3.12/PBS3 in complex with chorismate

To date, three-dimensional x-ray crystal structures of AtGH3.12/PBS3 have been solved in complex with AMP, AMP and SA, and a non-hydrolyzable ATP analog and SA (10, 28). Interestingly, the active site pocket space is bigger than SA, which suggested a possible larger substrate for the enzyme (10, 28). To gain an understanding of how chorismate potentially fits in the acyl acid binding pocket of AtGH3.12/PBS3, the 1.94 Å resolution x-ray crystal structure of the protein in complex with chorismate and AMP was solved by molecular replacement (**Table 3**).

The overall structure of the AtGH3.12/PBS3•chorismate•AMP complex was similar as the previously solved structures with the C-terminal flexible domain adopting the 'closed' active site conformation (**Fig. 5a**). Within the active site, clear electron density for AMP was observed, as was weaker, but interpretable, electron density for chorismate (**Fig. 5b**). The position of chorismate in the structure was in the same area of the active site as SA in the earlier structures (10, 28). Compared to other phytohormones or hormone analogues, including jasmonyl-isoleucine, a non-hydrolyzable IAA-AMP analogue, SA, and IAA, that have been co-crystallized with various GH3 proteins (10-13, 28, 30), chorismate contains multiple polar and charged moieties.

In the AtGH3.12/PBS3 active site, chorismate is oriented with the ring carboxylate pointed toward the phosphate group of the bound AMP molecule (**Fig. 5c**). This carboxylate forms charge-charge interactions with the side-chain of Arg123. An additional hydrogen bonding interaction occurs via a water-mediated contact with Tyr120. Ile217 is positioned below the chorismate ring and fits into the ring pucker. The distal chorismate carboxylate forms charge-charge interactions with Arg213 and a hydrogen bond with Tyr181. Although it does not directly interact with chorismate, Tyr178 forms charge-charge interactions with the side-chain of Arg123 to position it to interact with the ring carboxylate of chorismate. This set of active site residues is also invariant in AtGH3.7, which is consistent with the use of chorismate as an acyl acid substrate of both enzymes.

This structure provides a view of how chorismate can bind in the acyl acid site of AtGH3.12/PBS3; however, the location of the ligand likely does not represent where it binds during catalysis, as the ring carboxylate of chorismate is ~10 Å away from the AMP. As noted for other GH3 protein structures (11-13), charge repulsion between the carboxylate of an acyl acid substrate and the nucleotide phosphate can alter positioning of ligands in the site. During the reaction sequence, the presence of Mg^{2+} is an essential counterion that balances active site charges and allows the first half-reaction to occur (10, 30-31).

Site-directed mutagenesis of AtGH3.12/PBS3 chorismate conjugation activity

To gain a better understanding of the contributions of residues in the acyl acid binding site of AtGH3.12/PBS3, several previously generated site-directed mutants (Y112F, Y120F, R123K, T161S, I217A, and F218Y) and three new point mutants (Y178F, Y181F, and R213K) were analyzed for their effect on steady-state kinetic parameters with chorismate (**Table 4**). The Y112F, T161S, and Y181F substitutions had modest <2.5-fold changes on catalytic efficiency (k_{cat}/K_m) compared to wild-type. As observed in the x-ray structure (**Fig. 5c**), these three residues are not in direct contact with the chorismate ligand. The Y120F mutant, which removes a hydrogen bond donor, displayed a 13.5-fold increase in K_m with a corresponding 22-fold reduction in catalytic efficiency. Mutation of

Arg123 to a lysine had a ~5-fold effect on k_{cat}/K_m. Mutations of the two residues at the boundary between the acyl acid and nucleotide binding sites - Ile217 and Phe218 - both impacted the activity of AtGH3.12/PBS3 with chorismate. The I217A mutant decreased k_{cat}/K_m nearly 50-fold with a combination of increased K_m and reduced turnover rate. The effects of the F218Y mutant was comparable with an 18-fold decrease in catalytic efficiency.

With chorismate bound in the structure, several residues that were not previously analyzed emerged as potential mutagenesis targets - Tyr178, Tyr181, and Arg213. At the distal side of the bound chorismate, each tyrosine was mutated to phenylalanine. The Y181F mutant exhibited a less than 2-fold effect on catalytic efficiency (**Table 4**); however, the Y178F substitution, which removes a positioning interaction with Arg213, had no detectable activity (**Table 4)**. Likewise, the R213K variant was inactive. These results suggest that the combination of Tyr178 and Arg213 are critical for the chorismate-conjugation activity of AtGH3.12/PBS3.

Arabidopsis *gh3.7* mutants show wild-type pathogen response when infected with *PstDC3000*

Because AtGH3.7 and AtGH3.12/PBS3 can both use chorismate as a substrate, we hypothesized that the two proteins could have redundant and/or overlapping functions *in planta*. Previous physiological investigations of *gh3.12*/*pbs3* knockout mutants in Arabidopsis showed that the gene was involved in pathogen defense, and the knockout showed enhanced disease susceptibility to virulent and avirulent strains of *P. syringae* pv. tomato DC3000 (14-17). Moreover, *gh3.12/pbs3* mutants are compromised in pathogen-induced SA-glucoside accumulation, and this accumulation could be restored by exogenous application of SA, which also enhanced resistant to virulent *P. syringae* DC3000 (17).

Here we infected *gh3.7-1* mutants by leaf syringe infiltration with wild-type *P. syringae* DC3000 and found no statistically significant difference between wild-type and mutant plants (**Fig. 6**). The Arabidopsis *isochorismate synthase* mutant, *sid2-2*, was included as a positive control because it shows enhanced disease symptoms and is more susceptible to pathogen infection (18). In contrast, to *gh3.7-1* mutants *gh3.12/pbs3* mutant plants were significantly more susceptible to *P. syringae* DC3000 on day 4 ($p < 0.0001$), as was *sid2-2* ($p = 0.012$). This confirmed that AtGH3.7 has a different role than AtGH3.12/PBS3 in defending aerial tissue against pathogens. This result suggests that the product of AtGH3.12/PBS3 may be important for pathogen resistance, while the product of GH3.7 appears to not be involved. There was no visible growth phenotype in the *gh3.7-1* plants compared to wild-type Arabidopsis plants.

Arabidopsis *gh3.7 gh3.12* double mutants are more susceptible to infection than wild-type

While *gh3.7-1* had neither a disease resistance nor a pathogen susceptibility phenotype, a double mutant *A. thaliana* line was generated by crossing *gh3.7-1* and *gh3.12/pbs3* mutant lines. Overall, there were no noticeable growth phenotypes between the *gh3.7-1 gh3.12/pbs3* double mutant and wild-type plants. Also, to confirm that *gh3.7-1* knockout lines showed wild-type pathogen responses, a second allele was included in these experiments, *gh3.7-2*. Plants were infected by syringe infiltration using wild-type *P. syringae* DC3000, and *sid2-2* was included as a positive control. In these experiments, *gh3.7-2* showed some resistance to *P. syringae* DC3000 compared to wild-type, but this difference was not statistically significant ($p = 0.33$) (**Fig. 7**). Therefore, AtGH3.7 and

AtGH3.12/PBS3 do not have evidently redundant roles in pathogen responses in infected leaf tissue. On day 4 after infection, the *gh3.7-1 gh3.12/pdb3* double mutant was more susceptible to infection compared to wild-type ($p < 0.0001$) and was more susceptible compared to *gh3.12/pbs3* ($p < 0.0001$) and *sid2-2* ($p < 0.0001$) knockout lines (**Fig. 7**). This suggests that while AtGH3.7 alone does not function in defense in leaf tissues, the combination of both AtGH3.7 and AtGH3.12/PBS3 aids plants in pathogen response.

DISCUSSION

The GH3 family of acyl acid amido synthetases found in all plants is critical for modulating the concentration of acyl acid hormones in plants by conjugating them to amino acids (2-3). AtGH3.12/PBS3, was previously shown to conjugate glutamate to 4-HBA, which is not a plant hormone (15). When AtGH3.12/PBS3 was first discovered, it was found to have an SA-deficiency phenotype that could be rescued by exogenous SA, which suggested that the enzyme works upstream of SA signaling (16-17). Recent work identified AtGH3.12/PBS3 as essential for isochorismate-derived biosynthesis of SA (24).

With this knowledge, we screened aromatic and aromatic precursor metabolites as substrates for AtGH3.12/PBS3 and for the previously uncharacterized AtGH3.7, a homologue of AtGH3.12/PBS3. This approach identified chorismate-conjugating activity for each protein (**Figs. 1-3; Tables 1-2**). Re-screening of AtGH3.12/PBS3 revealed that it had higher activity with chorismate than with 4-HBA and can conjugate chorismate to glutamate (**Figs. 1-2; Table 1**). Likewise, biochemical analysis of AtGH3.7, which is from the same clade of GH3 proteins in Arabidopsis (10), identified a similar chorismate conjugating activity with cysteine as the amino acid substrate (**Fig. 3**). Interestingly, despite the 75% amino acid sequence identity and use of the same acyl-acid substrate, SA inhibited AtGH3.12/PBS3 with a 340-fold lower IC_{50} value than that of AtGH3.7. Although recent analysis of the isochorismate conjugation activity of AtGH3.12/PBS3 suggests this as the major function of the enzyme (24), the use of commercially-available chorismate (in contrast to the unstable isochorismate molecule) for structure-function studies remains a valuable tool. Moreover, the potential role of AtGH3.7 as an isochorismate-conjugating enzyme remains to be examined.

The GH3 acyl acid amido synthetases follow a two-step ping-pong mechanism where the acyl acid substrate binds and is adenylated and pyrophosphate is released, followed by a transfer step where the amino acid is added to the acyl acid to form the conjugate and AMP is released (10, 30). This mechanism helps explain why 4-HBA was identified as a substrate of AtGH3.12/PBS3. Early assays only measured pyrophosphate release in the first half-reaction (15). The assay used to identify chorismate as a substrate measured AMP release after the full reaction sequence. As noted here (**Fig. 4**), the difference between pyrophosphate release from the 4-HBA and chorismate reactions in the absence and presence of an amino acid substrate (i.e., glutamate) with AtGH3.12/PBS3 suggests that the substrates are held in the active site until the amino acid transferase step. This is a similar mechanism to ensure proper product formation as observed in other adenylating enzymes (32-33).

Having chorismate bound in a structure provided further evidence that chorismate is preferred over 4-HBA as a substrate of AtGH3.12/PBS3 (**Fig. 5**). Compared to the x-ray crystal structures of other GH3 acyl acid amido synthetase that use either auxins or jasmonic acid, key differences among the structures reveal how the AtGH3.12/PBS3

active site recognizes chorismate (10-13, 28-29). The active site of AtGH3.11/JAR1 has only one polar residue, a histidine, that interacts with the jasmonic acid ketone through a water molecule (10). The auxin-conjugating GH3 proteins have polar residues situated to interact with their substrates (11-13, 28-29). In comparison, the AtGH3.12/PBS3 active site contains two arginines and two tyrosines, with one of each positioned near each carboxylate of chorismate (**Fig. 5**). As indicated by kinetic analysis of site-directed mutants of AtGH3.12/PBS3 (**Table 4**), the charge-charge interactions between the arginines and the carboxylates appear critical for positioning chorismate or isochorismate in the active site for the ensuing adenylation and amino acid transfer reactions.

Considering that amino acid sequence identity of AtGH3.12/PBS3 and AtGH3.7, we wondered if they would have physiologically redundant roles *in planta*. Because AtGH3.12/PBS3 has an SA-deficiency response and both proteins can use chorismate as an acyl-acid substrate, we hypothesized that the enzyme products may have similar roles in pathogen defense. To determine the role of AtGH3.7 in pathogen defense, knockout lines were infected with *P. syringae.* Next, we examined if the roles of AtGH3.7 and AtGH3.12/PBS3 were additive and generated an Arabidopsis double mutant. The *gh3.7-1 gh3.12* double mutants were even more susceptible to pathogen infection than *gh3.12* mutants alone and than the positive control, the *isochorismate synthase sid2-2* knockout line, which is deficient in SA biosynthesis (**Fig. 7**). This suggests that having both AtGH3.7 and AtGH3.12/PBS3 is important in Brassicaceae species for defense against pathogenic microorganisms.

Knowing the promiscuous biochemical activity of AtGH3.12/PBS3 presents several possibilities for the role of the chorismate-related metabolites *in planta*. In the absence of this protein, plants are more susceptible to pathogen attack and were found to have less SA-glucoside accumulation after infection (15-17). This data suggests that the enzyme is upstream of SA biosynthesis, as was confirmed for the isochorismate-glutamate conjugates that spontaneously degrade into SA (24). One possibility is that chorismate-glutamate is siphoning chorismate away from other biosynthetic pathways, including that of the auxins IAA and phenylacetic acid as a storage form of the molecule; however, a hydrolase that would release free chorismate remains to be identified.

Both AtGH3.12/PBS3 and AtGH3.7 are cytoplasmic proteins (as each has no clear chloroplast localization sequence), while SA biosynthesis occurs in the plastid of plants (18). How chorismate is transferred from the chloroplast is an open question as a chorismate transporter has yet to be identified. Evidence now suggests that EDR5 (Enhanced Disease Susceptibility5) transports isochorismate from the plastid to the cytosol (24), which raises the possibility of this protein as a transporter of chorismate, as well.

Interestingly, AtGH3.12/PBS3 and AtGH3.7 are not the only cytosolic enzymes that can use chorismate as a substrate; chorismate mutase 2 in Arabidopsis is found in the cytosol and converts chorismate into prephenate, the precursor to tyrosine and phenylalanine via the arogenate pathway (34-38). The chorismate-conjugates could be diverting chorismate from the cytosolic chorismate mutase that would convert it into prephenate. There may be separate, non-redundant physiological roles for the two conjugates *in planta.* Future studies are needed to decipher the function of these metabolites in pathogenesis in Brassicaceae.

In conclusion, we have identified chorismate, a hormone biosynthetic intermediate, as a substrate for the Brassicaceae-specific clade of GH3 proteins that contains AtGH3.7 and AtGH3.12/PBS3.

Although AtGH3.12/PBS3 was previously shown to be involved in pathogen defense responses (15-17, 24), the physiological role and potential isochorismate conjugationg activity of AtGH3.7 remains to be understood as it does not exhibit a statistically significant effect during pathogen attack, suggesting a different role from AtGH3.12/PBS3. Taken together, these data suggest that regulation and modification of SA biosynthetic intermediates is a critical component of pathogen responses in the Brassicaceae.

EXPERIMENTAL PROCEDURES

Protein expression and purification

The pET-28a-AtGH3.12/PBS3 construct was previously described (10). The *E. coli* codon-optimized pET-28a-AtGH3.7 was ordered from Genewiz. For protein expression, pET-28a-AtGH3.12/PBS3 and pET28a-AtGH3.7 were transformed into the Rosetta2 (DE3) cells (Novagen). Protein expression was induced with 1 mM isopropyl β-D-1-thiogalactopyranoside for 15-18 hours at 18°C. Cells were lysed by sonication, and proteins were purified using a Ni^{2+}-nitrilotriacetic acid (Qiagen) column equilibrated in the lysis buffer (50 mM Tris (pH 8.0), 500 mM NaCl, 20 mM imidazole, 10% glycerol, and 1% Tween-20). The column was then washed with 50 mM Tris (pH 8.0), 500 mM NaCl, 20 mM imidazole, and 10% glycerol, and bound His-tagged protein was eluted with wash buffer containing 250 mM imidazole. Protein concentration was determined by the Bradford method (Bio-Rad) with bovine serum albumin as standard. For protein crystallography, AtGH3.12/PBS3 was then further purified by size-exclusion chromatography using a Superdex-75 26/60 HiLoad ÄKTA FPLC size-exclusion column (GE Healthcare) equilibrated with 50 mM Tris (pH 8.0) and 100 mM NaCl. Mutants were either from previous work or generated using the Quikchange PCR method (Strategene) with expression and purification as above.

Enzyme assays

Activity assays were performed using an enzyme coupled system containing 10 units of myokinase, pyruvate kinase, and lactate dehydrogenase, 1 mM phosphoenolpyruvate, and 1 mM NADH to couple AMP generation to conversion of NADH to NAD^+, which leads to a decrease in absorbance at 340 nm (30). Reaction mixtures contain 2 mM ATP, 2 mM $MgCl_2$, 0-2 mM acyl acid, 0-10 mM amino acid, and purified AtGH3.12/PBS3 (1 μg) or AtGH3.7 (10 μg). For assays with chorismate, the substrate was isolated and characterized as previously described (38). For determination of kinetic parameters, reactions were performed with either 4-HBA or chorismate varied from 0 - 1 mM. All data were fit to the Michaelis-Menten equation using GraphPad Prism. Inhibition of AtGH3.12/PBS3 and AtGH3.7 was analyzed using 10 μg of protein with 1 mM chorismate and 10 mM amino acid (glutamate or cysteine for AtGH3.12/PBS3 or AtGH3.7, respectively) in the presence of varied (0-10 mM) SA. IC_{50} values were determined by fitting data to $y = max / (1 + (I_f / IC_{50}))$, where max is the maximum observed rate difference and I_f is the inhibitor concentration, in GraphPad Prism.

Mass spectrometry

To confirm chorismate-glutamate conjugate formation, reaction assays were performed at 25 °C with 1 mM ATP, 1 mM $MgCl_2$, 1 mM chorismate, 5 mM glutamate, 50 mM Tris pH 8.0, and 100 μg AtGH3.12/PBS3 in 500 μl. Control reactions without protein (or each substrate) were also performed. Reactions were quenched with 50% (v/v) acetonitrile and 0.1% (v/v) acetic acid. Samples were analyzed by LC-MS/MS as previously described (39).

Pyrophosphate release assays

Adenylation assays were performed using the pyrophosphate reagent assay kit (Sigma-Aldrich) to couple pyrophosphate release to NADH depletion with 2 mM ATP, 2 mM $MgCl_2$, and purified AtGH3.12/PBS3 (30 μg) with either 4-HBA or chorismate (1 mM) in the absence or presence of glutamate (10 mM) (15). Assays were performed at 25 °C and were initiated by the addition of enzyme.

Protein crystallography

Crystals of AtGH3.12/PBS2 in complex with AMP and chorismate were grown by the vapor diffusion method in hanging drops of a 1:1 mixture of protein (15 mg ml^{-1}) and crystallization buffer (15% PEG-3350 (w/v), 0.25 M ammonium acetate, 100 mM sodium acetate (pH 4.4), 5 mM tris(2-carboxyethyl)phosphine, 5 mM $MgCl_2$, 10 mM chorismate, and 4 mM AMP). Crystals were flash frozen with mother liquor supplemented with 30% PEG-3350 as a cryoprotectant. Diffraction data was collected at ESRF ID23-2 and were indexed and integrated with XDS and scaled with XSCALE (40-41). Molecular replacement was performed with PHASER (42) using the previously solved AtGH3.12 structure (PDB: 4EQL; 10) for the search model. Structures were refined with BUSTER (43) and manual model building was done in COOT (44). Data collection and refinement statistics are shown in **Table 3**. Coordinates and structure factors for AtGH3.12/PBS3 in complex with AMP and chorismate were deposited in the PBD (PDB: 6OMS).

Plant and pathogen materials and growth conditions

All *Arabidopsis thaliana* transgenic lines and mutants used in this study were in the Col-0 background. The *sid2-2* mutant (18) was obtained from Barbara Kunkel. Plants were grown on soil in a growth chamber with a short-day photoperiod (8 h light/16 h dark) at 21°C with a relative humidity of 75% and a light intensity of ~130 μEinsteins sec^{-1} m^{-1}. *P. syringae* strain DC3000 (45) were grown on Nutrient Yeast Glycerol medium (NYG) at 28°C (46). The *gh3.7 gh3.12* double mutant was generated using *gh3.7* SALK_106726 and *gh3.12* SALK_018225C lines as parents in the crosses (47). PCR verified that each SALK line and the double-mutant were knockout lines. To confirm the phenotype of *gh3.7*, the SAIL_755_E09 line was also used in plant infection experiments.

***P. syringae* inoculation and quantification of bacterial growth**

Leaves of five-week old *A. thaliana* plants were infected by syringe infiltrations using a solution containing 10^5 cells ml^{-1} in 10 mM $MgCl_2$ and a 1-ml needleless syringe. To quantify bacterial growth in the plant, whole leaves were sampled at days zero, two, and four post-inoculation, weighed to determine leaf mass (mg), ground in 10 mM $MgCl_2$, and then plated in serial dilutions on NYG media supplemented with rifampicin. Between four and six leaves were sampled per treatment (48).

ACKNOWLEDGEMENTS

This work was supported by NSF grant MCB-1614539 to J.M.J. C.K.H. was supported by the NSF Graduate Research Fellowship Program (DGE-1143954), and C.S.W. was supported by a U.S. Department of Agriculture National Institute of Food and Agriculture predoctoral fellowship (MOW-2010-05240). A.D.S. was supported by the Howard Hughes Medical Institute Exceptional Research Opportunities Program. Portions of this research were carried out at the European Synchrotron Radiation Facility.

CONFLICT OF INTEREST

The authors declare that they have no

conflicts of interest with the contents of this article.

REFERENCES

1. Santer, A., Calderon-Villalobos, L.I.A., Estelle, M. (2009) Plant hormones are versatile chemical regulators of plant growth. *Nature Chem. Biol.* **5**, 301-307
2. Westfall, C.S., Muehler, A.M., Jez, J.M. (2013) Enzyme action in the regulation of plant hormone responses. *J. Biol. Chem.* **288**, 19304-19311
3. Korasick, D.A., Enders, T.A., Strader, L.C. (2013) Auxin biosynthesis and storage forms. *J. Exp. Bot*. **64**, 2541-2555
4. Hagen, G., Guilfoyle, T.J. (1985) Rapid induction of selective transcription by auxins. *Mol. Cell. Biol.* **5**, 1197-1203
5. Feys, B.J.F., Benedetti, C.E., Penfold, C.N., Turner, J.G. (1994) Arabidopsis mutants selected for resistance to the phytotoxin coronatine are male sterile, insensitive to methyl jasmonate, and resistant to a bacterial pathogen. *Plant Cell* **6**, 751-759
6. Xie, D., Feys, B.F., James, S., Nieto-Rostro, M., Turner, J.G. (1998) COI1: An Arabidopsis gene required for jasmonate-regulated defense and fertility. *Science* **280**, 1091-1094
7. LeClere, S., Tellez, R., Rampey, R.A., Matsuda, S.P., Bartel, B. (2002) Characterization of a family of IAA-amino acid conjugate hydrolases from Arabidopsis. *J. Biol. Chem.* **277**, 20446-20452
8. Staswick, P.E., Tiryaki, I., Rowe, M.L. (2002) Jasmonate response locus JAR1 and several related Arabidopsis genes encode enzymes of the firefly luciferase superfamily that show activity on jasmonic, salicylic, and indole-3-acetic acids in an assay for adenylation. *Plant Cell* **14**, 1405-1415
9. Staswick, P.E., Serban, B., Rowe, M., Tiryaki, I., Maldonado, M.T., Maldonado, M.C., Suza, W. (2005) Characterization of an Arabidopsis enzyme family that conjugates amino acids to indole-3-acetic acid. *Plant Cell* **17**, 616-627
10. Westfall, C.S., Zubieta, C., Herrmann, J., Kapp, U., Nanao, M.H., Jez, J.M. (2012) Structural basis for prereceptor modulation of plant hormones by GH3 proteins. *Science* **33**, 1708-1711
11. Westfall, C.S., Sherp, A.M., Zubieta, C., Alvarez, S., Schraft, E., Marcellin, R., Ramirez, L., Jez, J.M. (2016) Arabidopsis thaliana GH3.5 acyl acid amido synthetase mediates metabolic crosstalk in auxin and salicylic acid homeostasis. *Proc. Natl. Acad. Sci. USA* **113**, 11917-11922
12. Sherp, A.M., Westfall, C.S., Alvarez, S., Jez, J.M. (2018) *Arabidopsis thaliana* GH3.15 acyl acid amido synthetase has a highly specific substrate preference for the auxin precursor indole-3-butyric acid. *J. Biol. Chem*. **293**, 4277-4288
13. Sherp, A.M., Lee S.G., Schraft, E., Jez, J.M. (2018) Modification of auxinic phenoxyalkanoic acid herbicides by the acyl acid amido synthetase GH3.15 from Arabidopsis. *J. Biol. Chem.* **293**, 17731-17738.
14. Warren, R.F., Merritt, P.M., Holub, E., Innes, R.W. (1999) Identification of three putative signal transduction genes involved in R gene-specified disease resistance in Arabidopsis. *Genetics* **152**, 401-412
15. Okrent, R.A., Brooks, M.D., Wildermuth, M.C. (2009) Arabidopsis GH3.12 (PBS3) conjugates amino acids to 4-substituted benzoates and is inhibited by salicylate. *J. Biol. Chem.* **284**, 9742-9754
16. Jagadeeswaran, G., Raina, S., Acharya, B.R., Maqbool, S.B., Mosher, S.L., Appel, H.M.,

Schultz, J.C., Klessig, D.F., Raina, R. (2007) Arabidopsis GH3-like defense gene 1 is required for accumulation of salicylic acid, activation of defense responses and resistance to *Pseudomonas syringae*. *Plant J.* **51**, 234-246

17. Nobuta, K., Okrent, R.A., Stoutemyer, M., Rodibaugh, N., Kempema, L., Wildermuth, M.C., Innes, R.W. (2007) The GH3 acyl adenylase family member PBS3 regulates salicylic acid-dependent defense responses in Arabidopsis. *Plant Physiol.* **144**, 1144-1156
18. Wildermuth, M.C., Dewdney, J., Wu, G., Ausubel, F.M. (2001) Isochorismate synthase is required to synthesize salicylic acid for plant defence. *Nature* **414**, 562-571
19. Strawn, M.A., Marr, S.K., Inoue, K., Inada, N., Zubieta, C., Wildermuth, M.C. (2007) Arabidopsis isochorismate synthase functional in pathogen-induced salicylate biosynthesis exhibits properties consistent with a role in diverse stress responses. *J. Biol. Chem.* **282**, 5919-5933
20. Garcion, C., Lohman, A., Lamodi`ere, E., Catinot, J., Buchala, A., Doermann, P., Metreaux, J.-P. (2008) Characterization and biological function of the ISOCHORISMATE SYNTHASE 2 gene of Arabidopsis thaliana. *Plant Physiol.* **147**, 1279-1287
21. Dean, J.V., Mills, J.D. (2004) Uptake of salicylic acid 2-O-β-D-glucose into soybean tonoplast vesicles by an ATP-binding cassette transporter-type mechanism. *Physiol Plant.* **120**, 603-612
22. Dean, J.V., Mohammed, L.A., Fitzpatrick, T. (2005) The formation, vacuolar localization, and tonoplast transport of salicylic acid glucose conjugates in tobacco cell suspension cultures. *Planta* **221**, 287-296
23. Hennig, J., Malamy, J., Grynkiewicz, G., Indulski, J., Klessig, D.F. (1993) Interconversion of the salicylic acid signal and its glucoside in tobacco. *Plant J.* **4**, 593-600
24. Rekhter, D., Lüdke, D., Ding, Y., Feussner, K., Zienkiewicz, K., Lipta, V., Wiermer, M., Zhang, Y., Feussner, I. (2019) Isochorismate-derived biosynthesis of the plant stress hormone salicylic acid. *Science* **365**, 498-502
25. Vlot, A.C., Dempsey, D.A., Klessig, D.F. (2009) Salicylic acid, a multifaceted hormone to combat disease. *Annu. Rev. Phytopathol.* **47**, 177-206
26. Mauch-Mani, B., Slusarenko, A.J. (1996) Production of salicylic acid precursors is a major function of phenylalanine ammonia-lyase in the resistance of Arabidopsis to *Peronospora parasitica*. *Plant Cell* **8**, 203-212
27. Serino, L., Reimmann, C., Baur, H., Beyeler, M., Visca, P., Haas, D. (1995) Structural genes for salicylate biosynthesis from chorismate in *Pseudomonas aeruginosa*. *Mol. Gen. Genet*. **249**, 217-228
28. Round, A., Brown, E., Kapp, U., Marcelin, R., Westfall, C.S., Pernot, P., Jez, J.M., Zubieta, C. (2013) Determination of GH3.12 protein conformation through on-line HPLC-integrated SAXS measurements combined with x-ray crystallography. *Acta Crystallogr. D* **69**, 2072-2080
29. Peat, T.S., Böttcher, C., Newman, J., Lucent, D., Cowieson, N., Davies, C. (2012) Crystal structure of an indole-3-acetic acid amido synthetase from grapevine involved in auxin homeostasis. *Plant Cell* **24**, 4528-4538
30. Chen, Q., Westfall, C.S., Hicks, L.M., Wang, S., Jez, J.M. (2010) Kinetic basis for the conjugation of auxin by a GH3 family indole acetic acid-amido synthetase. *J. Biol. Chem.* **285**, 29780-29786

31. Westfall, C.S., Herrmann, J., Chen, Q., Wang, S., Jez, J.M. (2010) Modulating plant hormone levels by enzyme action: the GH3 family of acyl acid amido synthetases. *Plant Signal. Behav.* **5**, 1597-1602
32. Yadavalli, S.S., Ibba. M. (2012) Quality control in aminoacyl-tRNA synthesis its role in translational fidelity. *Adv. Protein Chem. Struct. Biol.* **85**, 1-43
33. Manandhar, M., Cronan, J.E. (2013) Proofreading of noncognate acyl adenylates by an acyl-coenzyme a ligase. Chem. Biol. **20**, 1441-1446
34. Eberhard, J., Ehrler, T.T., Epple, P., Felix, G., Raesecke, H.R., Amrhein, N., Schmid, J. (1996) Cytosolic and plastidic chorismate mutase isozymes from *Arabidopsis thaliana*: molecular characterization and enzymatic properties. *Plant J.* **10**, 815-821
35. Mobley, E.M., Kunkel, B.N., Keith, B. (1999) Identification, characterization, and comparative analysis of a novel chorismate mutase gene in Arabidopsis thaliana. *Gene* **240**, 115-123
36. Colquhoun, T.A., Schimmel, B.C., Kim, J.Y., Reinhardt, D., Cline, K., Clark, D.G. (2010) A petunia chorismate mutase specialized for the production of floral volatiles. *Plant J.* **61**, 145-155
37. Westfall, C.S., Xu, A., Jez, J.M. (2014) Structural evolution of differential amino acid effector regulation in plant chorismate mutases. *J. Biol. Chem.* **289**, 28619-28628
38. Kroll, K., Holland, C.K., Starks, C.M., Jez, J.M. (2017) Evolution of allosteric regulation in chorismate mutases from early plants. *Biochem. J.* **474**, 3705-3717
39. Chen, Q., Zhang, B., Hicks, L.M., Wang, S., Jez, J.M. (2009) A liquid chromatography-tandem mass spectrometry-based assay for indole-3-acetic acid-amido synthetases. *Anal. Biochem.* **390**, 149-154
40. Kabsch, W. (2010) XDS. *Acta Crystallogr. D* **66**, 125-132
41. Sheldrick, G.M. (2008) A short history of SHELX. *Acta Crystallogr. A* **64**, 112-122
42. de la Fortelle, E., Bricogne, G. (1997) Maximum-likelihood heavy-atom parameter refinement for the multiple isomorphous replacement and multiwavelength anomalous diffraction methods. *Methods Enzymol.* **276**, 472-494
43. Blanc, E., Roversi, R., Vonrhein, C., Flensburg, C., Lea, S.M., Bricogne, G. (2004) Refinement of severely incomplete structures with maximum likelihood in BUSTER-TNT. *Acta Crystallogr. D* **60**, 2210-2221
44. Emsley, P., Cowtan, K. (2004) Coot: model-building tools for molecular graphics. *Acta Crystallogr. D* **60**, 2126-2132
45. Cuppels, D.A. (1986) Generation and Characterization of Tn5 Insertion Mutations in *Pseudomonas syringae* pv. tomato. *Appl. Environ. Microbiol.* **52**, 323-327
46. Daniels, M.J., Barber, C.E., Turner, P.C., Sawczyc, M.K., Byrde, R.J.W., Fielding, A.H. (1984) Cloning of genes involved in pathogenicity of *Xanthomonas campestris* pv. *campestris* using the broad host range cosmid pLAFR1. *EMBO J.* **3**, 3323-3328
47. Alonso, J.M., Stepanova, A.N., Leisse, T.J., Kim, C.J., Chen, H., Shinn, P., Stevenson, D.K., Zimmerman, J., Barajas, P., Cheuk, R., Gadrinab, C., Heller, C., Jeske, A., Koesema, E., Meyers, C.C., Parker, H., Prednis, L., Ansari, Y., Choy, N., Deen, H., Geralt, M., Hazari, N., Hom, E., Karnes, M., Mulholland, C., Ndubaku, R., Schmidt, I., Guzman, P., Aguilar-Henonin, L., Schmid, M., Weigel, D., Carter, D.E., Marchand, T., Risseeuw, E., Brogden, D., Zeko, A., Crosby, W.L., Berry, C.C., Ecker, J.R. (2003) Genome-wide insertional

mutagenesis of *Arabidopsis thaliana.* *Science* **301**, 653-657

48. Laurie-Berry, N., Joardar, V., Street, I.H., Kunkel, B.N. (2006) The *Arabidopsis thaliana JASMONATE INSENSITIVE 1* gene is required for suppression of salicylic acid-dependent defenses during infection by *Pseudomonas syringae.* *Mol. Plant Micro. Interact.* **19**, 789-800

FOOTNOTE

Non-standard abbreviations used are: GH3, Gretchen Hagen 3; HBA, 4-hydroxybenzoic acid; IAA, indole-3-acetic acid; SA, salicylic acid

Table 1. Summary of steady-state kinetic parameters of AtGH3.12/PBS3. Assays were performed and kinetic parameters determined as described in the Experimental Procedures. Assays with varied concentrations of 4-HBA (0-1 mM) and chorismate (0-1 mM) used fixed concentrations of glutamate (10 mm) and ATP (2 mM). Assays with varied glutamate (0-10 mM) were performed at fixed concentrations of chorismate (1 mM) and ATP (2 mM). Values are averages ± SD (n = 3). Abbreviation: 4-HBA, 4-hydroxybenzoic acid.

varied substrate (fixed substrates)	k_{cat} (min^{-1})	K_m (μM)	k_{cat}/K_m (M^{-1} s^{-1})
4-HBA (glutamate, ATP)	4.5 ± 0.4	270 ± 50	278
chorismate (glutamate, ATP)	43 ± 3	170 ± 30	4,220
glutamate (chorismate, ATP)	220 ± 14	3,100 ± 500	1,180

Table 2. Summary of steady-state kinetics of AtGH3.7. Assays were performed and kinetic parameters determined as described in the Experimental Procedures. Assays with varied concentrations of chorismate (0-1 mM) used fixed concentrations of each noted amino acid (10 mm) and ATP (2 mM). Assays with varied amino acid (0-10 mM) were performed at fixed concentrations of chorismate (1 mM) and ATP (2 mM). Values are averages ± SD (n = 3).

varied substrate (fixed substrates)	k_{cat} (min^{-1})	K_m (μM)	k_{cat}/K_m (M^{-1} s^{-1})
chorismate (cysteine, ATP)	22 ± 4	280 ± 60	1,310
chorismate (serine, ATP)	9.4 ± 2.0	230 ± 60	681
chorismate (glutamine, ATP)	4.2 ± 0.9	80 ± 30	875
cysteine (chorismate, ATP)	18 ± 2	300 ± 50	1,000
serine (chorismate, ATP)	--	>10 mM	--
glutamine (chorismate, ATP)	--	>10 mM	--

Table 3. Summary of AtGH3.12/PBS3•AMP•chorismate complex crystallographic statistics. Values in parentheses are for highest-resolution shell.

Data Collection	
Space group	$P2_1$
Cell dimensions	*a* = 91.44 Å, *b* = 67.00 Å, *c* = 101.0 Å; β = 106.4°
Wavelength (Å)	0.979
Resolution (Å) (highest shell)	48.6 - 1.94 (2.01 - 1.94)
Reflections (total/unique)	303,672 / 85,974
Completeness (highest shell)	98.7% (94.3%)
$\langle I/\sigma \rangle$ (highest shell)	8.9 (1.8)
R_{sym} (highest shell)	15.6% (93.8%)
Refinement	
R_{cryst} / R_{free}	0.181 / 0.215
No. of protein atoms	7,847
No. of waters	813
No. of ligand atoms	88
R.m.s.d., bond lengths (Å)	0.007
R.m.s.d., bond angles (°)	1.05
Avg. B-factor (Å^2): protein, water, ligand	25.5, 34.5, 40.3
Stereochemistry: most favored, allowed, disallowed	97.7, 2.3, 0 %

Table 4. Steady-state kinetic analysis of AtGH3.12/PBS3 mutants with chorismate. Assays were performed and kinetic parameters determined as described in the Experimental Procedures. Kinetic parameters for wild-type protein from Table 1 are included here for comparison. Values are averages ± SD (n = 3).

protein	k_{cat} (min^{-1})	K_m (μM)	k_{cat}/K_m (M^{-1} s^{-1})
wild-type	43 ± 3	170 ± 30	4,220
Y112F	42 ± 2	290 ± 30	2,410
Y120F	27 ± 4	2,300 ± 450	196
R123K	70 ± 5	1,300 ± 100	897
T161S	28 ± 1	280 ± 40	1,670
Y178F	--	--	--
Y181F	74 ± 7	500 ± 10	2,470
R213K	--	--	--
I217A	9.2 ± 0.5	1,100 ± 160	140
F218Y	9.2 ± 0.5	650 ± 90	236

Figure 1. Identification of chorismate conjugation activity of AtGH3.12/PBS3. (a) Acyl acid activity of AtGH3.12/PBS3. Acyl acid conjugation activity was observed with each substrate with glutamate and ATP. (b) Amino acid activity screen of AtGH3.12/PBS3. Assays were performed in the presence of chorismate and ATP with each amino acid. Assay conditions were as described in the Experimental Procedures. All values are average ± SD (n = 3). Abbreviations: 4-HBA, 4-hydroxybenzoic acid; BA, benzoic acid; one-letter codes for each amino acid are used in panel b.

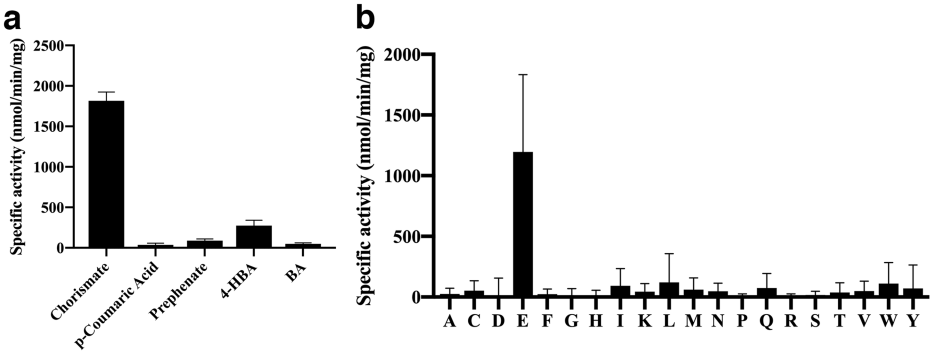

Figure 2. Mass spectrometry analysis of AtGH3.12/PBS3 chorismate conjugation activity. QTRAP LC-MS/MS fragmentation mass spectra (negative ion mode) of the chorismate-glutamate conjugate formed by AtGH3.12/PBS3 (deprotonated molecular ion ($M-H^-$) *m/z* = 353.9). Assay was performed as described in the Experimental Procedures.

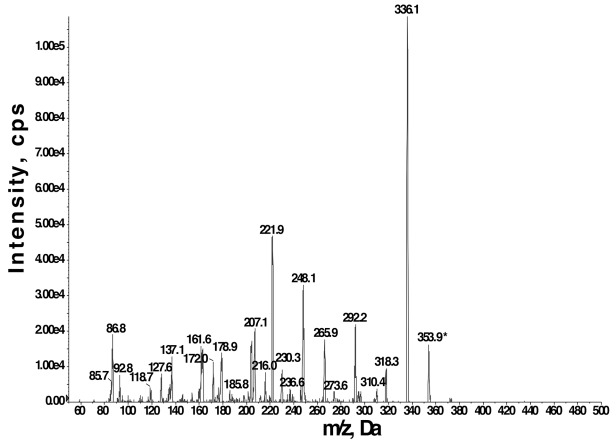

Figure 3. Identification of chorismate conjugation activity of AtGH3.7. (a) Acyl acid activity of AtGH3.7. Acyl acid conjugation activity was observed with each substrate with glutamate and ATP. (b) Amino acid activity screen of AtGH3.17. Assays were performed in the presence of chorismate and ATP with each amino acid. Assay conditions were as described in the Experimental Procedures. All values are average ± SD (n = 3). One-letter codes for each amino acid are used in panel b.

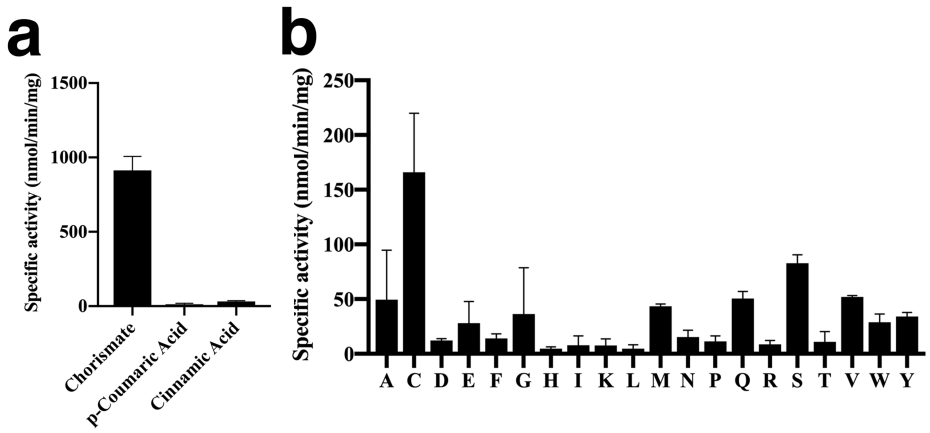

Figure 4. Adenylation activity of AtGH3.12/PBS3. The adenylation rate of AtGH3.12/PBS3 was measured with either 4-hydroxybenzoic (4-HBA) acid or chorismate in the absence or presence of glutamate (Glu). Values shown are average ± SD (n=3).

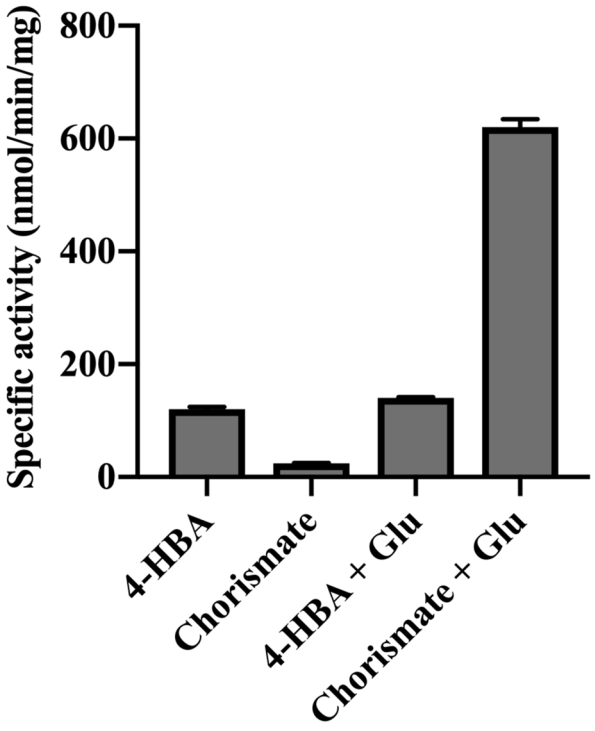

Figure 5. X-ray crystal structure of AtGH3.12/PBS3 in complex with chorismate and AMP. a) Overall structure. The ribbon diagram shows the N- and C-terminal domains of the protein with α-helices (blue) and β-strands (green) as cylinders and arrows, respectively. Chorismate and AMP are shown as space-filling models. b) Electron density for the ligands bound in the active site are shown as $2F_o$-F_c omit maps (1.0 σ). c) Active site view. Residues contacting the bound chorismate, as well as chorismate and AMP, are shown as stick models. d) Surface view of ligand binding in the active site. Chorismate and AMP are shown as stick models in the active site. Secondary structure and residues in the foreground were removed to provide a clearer view of the site.

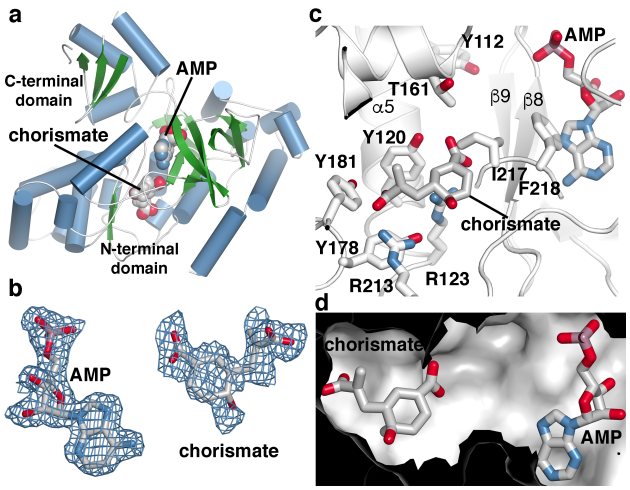

Figure 6. Arabidopsis *gh3.7-1* knockout lines do not have a pathogen infection phenotype. Leaves from infected plants were sampled 0, 2, and 4 days post-inoculation for quantifying *P. syrinagae* pv. tomato DC3000 growth in the tissue (colony forming units (CFU) / mg leaf; log-scale on the y-axis). a) This graph depicts three biological replicates with 4-6 leaves per replicate per genotype. Statistical analyses were conducted using a two-way ANOVA with statistical significance between control (wild-type; Col-O) and samples are indicated by asterisks (* = $p < 0.05$; **** = $p < 0.0001$). b) Zoomed-in view of day 4 data from panel a. All means were compared to all other means using a two-way ANOVA (**** = $p < 0.0001$).

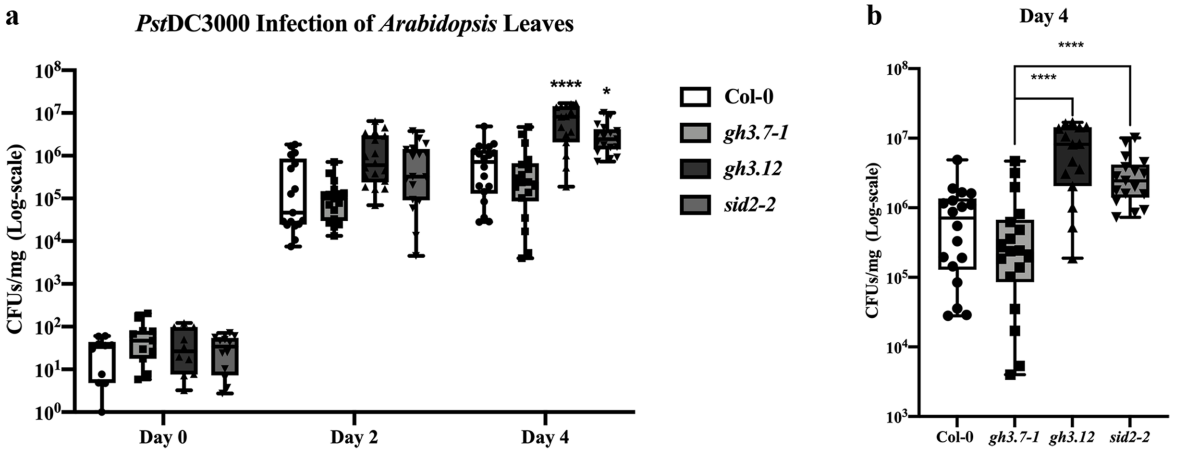

Figure 7. Arabidopsis *gh3.7-1 gh3.12/pbs3* double mutant lines are more susceptible to pathogen infection than wild-type or *sid2-2*. Leaves from infected plants were sampled 0, 2, and 4 days post-inoculation for quantifying *P. syrinagae* pv. tomato DC3000 growth in the tissue (colony forming units (CFU) / mg leaf; log-scale on the y-axis). a) This graph depicts four biological replicates with 4-6 leaves per replicate per genotype. Statistical analyses were conducted using a two-way ANOVA with statistical significance between control (wild-type; Col-O) and samples indicated by asterisks (**** = p <0.0001). b) Zoomed-in view of data from day 4 from panel a. All means were compared to all other means using a two-way ANOVA (**** = p <0.0001).

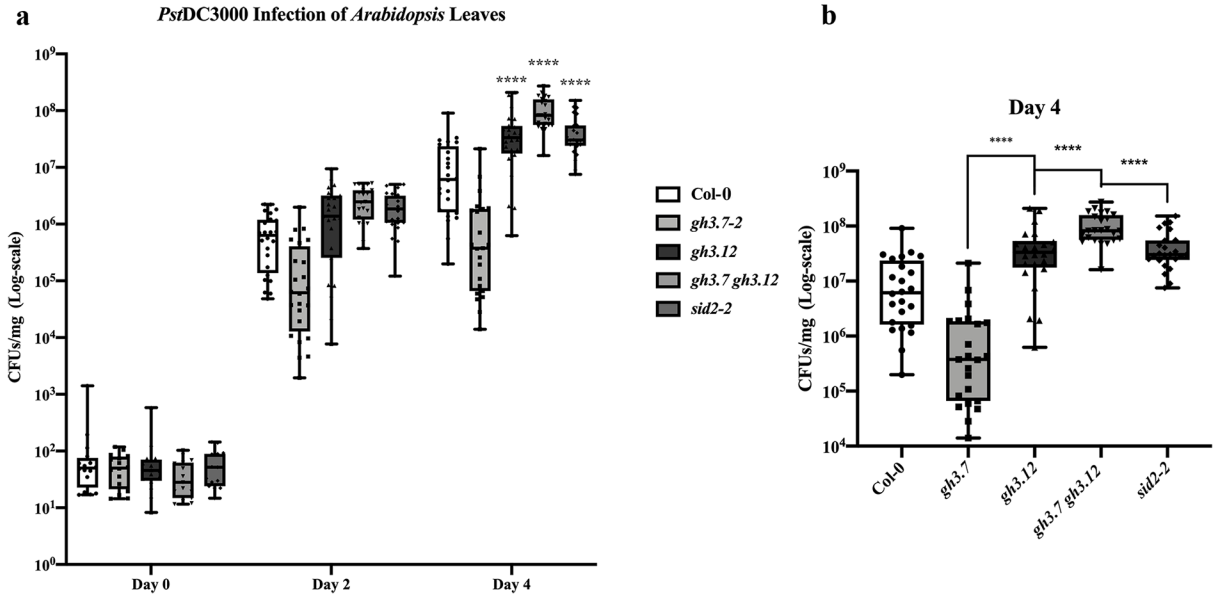

Brassicaceae-specific Gretchen Hagen 3 acyl acid amido synthetases conjugate amino acids to chorismate, a precursor of aromatic amino acids and salicylic acid

Cynthia K Holland, Corey S. Westfall, Jason E. Schaffer, Alejandro De Santiago, Chloe Zubieta, Sophie Alvarez and Joseph M. Jez

J. Biol. Chem. published online October 1, 2019
